Entanglement teleportation between distinct decohered qubits mediated via single and double Majorana wire(s)

Ngwa Engelbert Afuoti[1,2] ⓘ**, Lukong Cornelius Fai**[2]**, Ateuafack Mathurin**[2]**,
Georges Collince Fouokeng**[2,3] **and Jules Carsimir Ngana**[2,4]

[1] Department of Energy and Thermal Engineering, Douala University Institute of Technology, Douala, Cameroon
[2] Department of Physics, University of Dschang, Cameroon
[3] University Institute of Gulf of Guinea, Cameroon
[4] Department of Physics, University of Buea, Cameroon

E-mail: ngwaawah@yahoo.com

CrossMark

Abstract
We investigate the decoherence effects from a spin environment on two detached qubits coupled by a single Majorana wire (SMW) and double Majorana wires (DMWs) respectively when teleporting entanglement between the distinct qubits. The role of the composite system parameters on entanglement and entanglement teleportation are examined. Our results shows that strong coupling between the spin environment and the dots modifies the coupling between the qubits and the Majorana fermions (MFs) thus lifting the degenerate zero energy state for the case of the SMW. The SMW is seen to undergo a topological quantum phase transition as seen from the stable asymptotic increase and decrease in its dynamics as the coupling between the qubits and the MFs are varied. We observed that the DMWs are robust against quantum fluctuations of the spin environment with a characteristic cyclic beating phenomenon. This behavior shows that information is mediated via a channel endowed with the anti-ferromagnetic phase and the topological phase that harbors the Majorana zero-energy state. We probe the extent to which the capacitive and pure coupling that defines the DMWs should be tune for entanglement generation between the two sites and thus enhancement of the teleported state. Our description for the Majorana zero modes is in the spin model for spin based quantum applications.

Keywords: spin environment, qubits, single Majorana wire, double Majorana wires, entanglement, teleportation, fidelity

(Some figures may appear in colour only in the online journal)

1. Introduction

The quest for a protected channel during quantum state transfer between distinct quantum processors and registers has remain a challenge over the recent past years in the community of quantum computation and information processing technologies. The use of spin-chains and possible optimization techniques for enhancing its performances as a quantum channel [1–7] has been the subject of intense concerned recently. However for faithful quantum communication using the spin chain as channel, quantum engineers need to resolve a number of obstacles such as, decoherence arising from quantum fluctuations due to quasi-particle excitations within the chain, Dzyaloshinsky–Moriya interactions, chain length, external degrees of freedom or finite precision control changes the coupling strengths or induces energy fluctuations of the spins thus affecting the transfer fidelity and again when the quantum code to be transmitted suffers inevitable interactions with its host environment . All these require much quantum engineering resources. Among other proposals as quantum channels

[8–11], we consider in this paper a channel that in it is inherent the topological phase; a phase that is robust to local pertubations and has been reported to be useful in quantum computation and information processing protocols [12–15]. In condensed matter physics a topological phase features Majorana fermions (MFs) (quasi-particles that have neither a fermionic nor a bosonic character) if the hybrid system is rightly tuned [16–18]. MFs as quasi-particle excitations were anticipated to occur in different solid-state systems, such as the 5/2 fractional quantum Hall system [16], the p-wave superconductor [17] and the hybrid systems of a topological insulator [19]. Semiconductor nano-wire in proximity to an s-wave superconductor has recently been of great interest in the search for both theoretical and experimental exotic signatures of Majorana bound states (MBSs) [20–27]. In the quantum dot (QD) Majorana coupling settings [25], studied the quantum correlations between two spatially separate QDs induced by a pair of MFs emerging at the two ends of a semiconductor nanowire, in order to develop a new method for probing the MFs. They showed that the exotic nature of the MFs enhances entanglement even when the initial states are un-entangled. Ricco *et al* [28] investigated theoretically charge transport and heat tuning via MFs by considering a system of QD connected both to a pair of MFs residing at the edges of a Kitaev wire and two metallic leads. We consider a setup similar to that investigated in [24, 25, 27] where we call the single Majorana wire (SMW) but in different illumination. Here the remote dots (qubits) are buried in geographically detached but the same type of spin environment. This gives us room to address decoherence effects arising from quantum fluctuations from the sending and receiving environment during the teleportation of bipartite entanglement using a channel that support the topological phase. In the Majorana Wire setting, we consider that no interactions are made with the environment and thus no decoherence as a result of interaction between topological qubits and spin environment. The decoherence pattern of topological qubits couple to fermionic/bosonic Ohmic-like environment has been investigated in [26]. We further consider a configuration called the double Majorana wires (DMWs) as a bridge to route information between the remote qubits; a configuration that project the system to that of the macroscopic Kitaev's toy model [17], for Majorana wires when rightly tuned. As reported in [29], such a system with additional capacitive coupling between adjacent islands leads to an effective interaction between the Majorana modes and can be tuned to various phases, i.e. anti-ferromagnetic phase (AFM), paramagnetic phase (FM), topological phase and the floating phase, as the parameter space are varied. Studying quantum state teleportation over such a channel seems instructive as information can be driven through the various phases. This thus prepares the ground to investigate which channel; the SMW or DMWs is suitable for quantum state transfer.

The rest of the work is structured as follows; we provide the model describing the SMW as a bridge to teleport bipartite entanglement between two decohered qubits initially prepared in an arbitrary superposition of state that supports the Majorana end states in section 2.1 and subsequently that describing the DMWs in section 2.2. This paves the way for
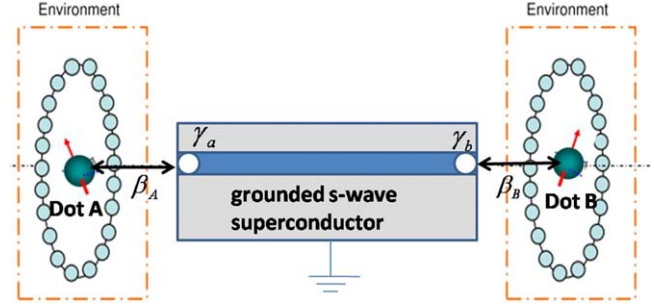
Figure 1. Schematic setup to probe quantum correlations and fidelity of entanglement teleportation between remote dots (qubits) mediated via a Majorana wire. The qubits are embedded in the same type of spin environment. The Majorana zero modes are represented by white dots.

the analytical derivation of the density matrices. The evaluation of concurrence, entanglement teleportation and average fidelity, for the respective configurations are carried out in section 3. The interpretation of the numerical results and conclusion forms the basis of sections 4 and 5 respectively.

2. Model Hamiltonian

2.1. Single Majorana wire (SMN)

We study a hybrid structure shown in figure 1, where a semiconductor nanowire with strong spin-orbit coupling with the conspiracy of pronounced Zeeman magnetic field and proximity-induced pairing correlations inherited from an s-wave superconducting substrate will induce the Majorana end states that are tunnel-coupled to two QDs, respectively. Two copies of the system below (figure 1) are used for transferring the entanglement as described in the Lee and Kim teleportation protocol [30]. The remote qubits are correlated only via the Majorana end states otherwise uncorrelated.

The remote QDs are considered to be in a single spin states (such that they can also be referred to as qubits) and are embedded in a spin bath permitting us to address decoherence effects on quantum correlations and entanglement teleportation. The Hamiltonian of the hybrid system can be written as

$$H_1 = H_{\text{sys}} + H_{D-E}. \tag{1}$$

The system Hamiltonian, H_{sys} describes the MBSs plus the single-level QDs and their tunnel coupling as follows [24, 25, 27]

$$H_{\text{sys}} = \sum_{j=A,B} [\varepsilon_j d_j^+ d_j + \beta_j(d_j^+ - d_j)\gamma_j] + \frac{i}{2}\varepsilon_m \gamma_A \gamma_B. \tag{2}$$

Here $d_A(d_A^+)$ and $d_B(d_B^+)$ and are the annihilation (creation) operators of the two single-level QDs, γ_A and γ_B are the Majorana operators associated with the two MBSs at the ends of the nanowire. The Majorana operators are Hermitian $\gamma_j = \gamma_j^+$ and fulfill the Clifford algebra $\{\gamma_i, \gamma_j\} = 2\delta_{ij}$; accounting for the fact that an isolated MBS is an equal superposition of electron

and hole excitations and therefore not a fermionic state. The two MBSs interact with each other by a strength $\varepsilon_M \approx e^{-L/\xi}$, which damps exponentially with the length L of the nanowire, ξ is the superconducting coherent length. β_A and β_B are the coupling amplitudes between Majorana end states and remote dots. For practical calculations, a transformation from the Majorana representation to the regular fermion one is necessary: $\gamma_A = i(f - f^+)$ and $\gamma_B = f + f^+$, with f and f^+ obeying the anti-commutation relation $\{f_i, f^+\} = 1$. After an additional local gauge transformation, $d_A \rightarrow id_A$, and $f \rightarrow if$, $f^+ \rightarrow -if^+$, we re-express equation (2) as

$$H_{\text{sys}} = \varepsilon_m\left(f^+ f - \frac{1}{2}\right) + \sum_{j=A,B} [\varepsilon_j d_j^+ d_j + \beta_j(d_j^+ f + f^+ d_j)]$$
$$- \beta_A(d_A^+ f + f d_A) + \beta_B(d_B^+ f + f d_B). \quad (3)$$

Equation (3) is further transformed into the spin model; recollecting in general that, $f = S^x - iS^y$, $f^+ = S^x + iS^y$ and $S^y = \frac{1}{2}\tau^y$, $S^x = \frac{1}{2}\tau^x$, thus

$$H_{\text{sys}} = \frac{\varepsilon_A}{2}\sigma_A^z + \frac{\varepsilon_B}{2}\sigma_B^z + \varepsilon_m\tau^z + \beta_A\sigma_A^y\tau^y + \beta_B\sigma_B^y\tau^y, \quad (4)$$

where $\sigma_A^z(\sigma_B^y)$ and $\tau^z(\tau^y)$ represents the Pauli spin operators for the right (left) dots (which may be regarded in this picture as two remote spins) and MFs respectively. For simplicity, we adopt a symmetric setup with $\beta_A = \beta_B = \beta$. Moreover, the two QDs are adjusted such that $\varepsilon_A = \varepsilon_B = \varepsilon$. For the new fermionic representation of the system Hamiltonain, H_{sys} equation (4), it is convenient to use the state basis $|n_A n_M n_B\rangle$ describing the possible spin configuration of the dot-Majorana-dot system, where $n_{A(B)}$ and n_M denotes, respectively, spin 'up' or 'down' in the right (left) and the central MBSs. We consider the following subspace with spin configuration: $|001\rangle$, $|010\rangle$, $|100\rangle$, $|111\rangle$ (a subspace with odd-parity for the corresponding charge configuration of the system Hamiltonian equation (3) [25]).

The Hamiltonian of the two remote spins transversely coupled to similar but separated spin environment, which is described by the one-dimensional *XY* model, is given by ($\hbar$ is taken to be unity)

$$H_{D-E} = -\sum_{l=1}^{N}\left(\frac{1+\alpha}{2}\sigma_l^x\sigma_{l+1}^x + \frac{1-\alpha}{2}\sigma_l^y\sigma_{l+1}^y + \lambda\sigma_l^z\right)$$
$$- \frac{g}{2}(\sigma_A^Z + \sigma_B^Z)\sum_{l=1}^{N}\sigma_l^z$$
$$\equiv H_E^{(\lambda)} + H_I, \quad (5)$$

where $H_E^{(\lambda)}$, given by the first line of equation (5) denotes the Hamiltonian of the environmental spin chain and H_I, given by the second line, describes the interaction between the two-qubit spins and the spin chain. The Pauli matrices $\sigma_l^\mu(\mu = x, y, z)$ are used to describe the spin chain of the environment. The parameter λ characterizes the intensity of the transverse magnetic field, and α measures the anisotropy in the in-plane interaction. The *XY* spin model described

by the first line in equation (5) encompasses other two spin models; the Ising spin chain with $\alpha = 1$ and the *XX* spin chain with $\alpha = 0$.

Using the result in [31] the diagonalized form of the Hamiltonian of the central two qubits dressed with the environment due to interaction is given by

$$H_E^{(\lambda_j)} = \sum_k \Omega_k^{(\lambda_j)}\left(b_{k,\lambda_j}^+ b_{k,\lambda_j} - \frac{1}{2}\right). \quad (6)$$

The absolute value of the decoherence factors is given as

$$|F_{mn}| = \prod_{k \succ 0} \begin{Bmatrix} 1 - \sin^2(2\alpha_k^{\lambda_m})\sin^2(\Omega_k^{\lambda_m}t) \\ - \sin^2(2\alpha_k^{\lambda_n})\sin^2(\Omega_k^{\lambda_n}t) \\ + 2\sin(2\alpha_k^{\lambda_m})\sin(\alpha_k^{\lambda_n}t)\sin(\Omega_k^{\lambda_m}t) \\ \times \sin(\Omega_k^{\lambda_n}t)\cos(\Omega_k^{\lambda_m}t - \Omega_k^{\lambda_n}t) \\ - 4\sin(2\alpha_k^{\lambda_m})\sin(2\alpha_k^{\lambda_n})\sin^2 \\ \times (\alpha_k^{\lambda_m} - \alpha_k^{\lambda_n})\sin^2(\Omega_k^{\lambda_m}t)\sin^2(\Omega_k^{\lambda_n}t) \end{Bmatrix}^{\frac{1}{2}}, \quad (7)$$

where the energy spectrum $\Omega_k^{(\lambda_j)}$ is given by $\Omega_k^{(\lambda_j)} = 2\sqrt{(\varepsilon_k^{(\lambda_j)})^2 + \alpha^2\sin^2\frac{2\pi k}{N}}$, with $\varepsilon_k^{(\lambda_j)} = \lambda_j - \cos\frac{2\pi k}{N}$. The parameters λ_j are $\lambda_{1(2)} = \lambda \pm g$, $\lambda_{3(4)} = \lambda$ corresponds to the dressed eigen-value due to interaction between the remote two spins and spin chain. $\alpha_k^{(\lambda_j)} = (\theta_k^{(\lambda_j)} - \theta_k^{(\lambda)})/2$ with angles, $\theta_k^{(\lambda_j)}$ satisfying, $\cos\theta_k^{(\lambda_j)} = 2\varepsilon_k^{(\lambda_j)}/\Omega_k^{(\lambda_j)}$. The energy spectrum $\Omega_k^{(\lambda_j)}$ carries information about all the possible excitations in the spin chain. Interaction between the spin chain and the qubits induces overlap between these excitations and thus quantum fluctuations.

The time evolving density matrix of the composite system may be written as

$$\rho(t) = \exp(-i(H_{\text{sys}} + H_E^{(\lambda_j)})t)\rho(0)$$
$$\times \exp(i(H_{\text{sys}} + H_E^{(\lambda_j)})t). \quad (8)$$

Considering that the initial density matrix of the composed system is separable, i.e. the preparation of the initial state of the central spin system takes place on a time scale much shorter than all the other characteristic time scales of the Hamiltonian, then, $\rho(0) = \rho_{AB}(0) \otimes \rho_E(0)$. $\rho_{AB}(0) = |\Phi(0)\rangle\langle\Phi(0)|$ is the density matrix of the central spins in the initial state, $|\Phi(0)\rangle$ is assume to be an initially prepared state of the systems Hamiltonian. Without lost of generality, we consider the initial spin configuration of the dot-MBSs-dot system to be in the following arbitrary superposition of state: $|\Phi\rangle = a|010\rangle + b|111\rangle$, with coefficients satisfying: $(a)^2 + (b)^2 = 1$. The density matrix, $\rho_E(0) = |\Psi(0)\rangle_E {}_E\langle\Psi(0)|$ describes the density matrix of the spin chain in the initial state, $|\Psi(0)\rangle_E$. Tracing the environmental degrees of freedom leads to the following equation

$$\rho(t) = \sum_{m,n,\mu,\nu=1}^{4} C_\mu^m \overline{C}_\nu^{*n} F_{mn}(t)|\varphi_\mu\rangle\langle\varphi_\nu|, \quad (9)$$

where $C_\mu^m = \exp(-iE_\mu t)\langle\varphi_\mu|\phi_m\rangle\langle\phi_m|\Phi\rangle$ and $\overline{C}_\nu^{*n} = \exp(iE_\nu t)$ $\langle\Phi|\phi_n\rangle\langle\phi_n|\varphi_\nu\rangle$. E_μ and $|\varphi_\mu\rangle$ are respectively the energy eigen-value and eigen vectors of the Hamiltonian equation (4).

We introduced the eigen-states, $|\phi_m\rangle$: $|010\rangle$, $|001\rangle$, $|100\rangle$, $|111\rangle$, of the interaction Hamiltonian to account for the fact that the system Hamiltonian, H_{sys} does not commute with the interaction Hamiltonian, H_I. After eliminating the degrees of freedom of the MFs, the reduced density matrix in the standard basis $\{|00\rangle, |01\rangle, |10\rangle, |11\rangle\}$ takes the X-structure

$$\rho_{AB}(t) = \begin{pmatrix} \rho_{11} & 0 & 0 & \rho_{14} \\ 0 & \rho_{22} & \rho_{23} & 0 \\ 0 & \rho_{32} & \rho_{33} & 0 \\ \rho_{14}^* & 0 & 0 & \rho_{44} \end{pmatrix}, \tag{10}$$

where:

$$\rho_{11} = (aA_1)^2 + (bA_4 R_1(E_4))^2 - 2A_1 A_4 ab R_1$$
$$\times (E_4)\cos((E_1 - E_4)t)F_{14},$$

$$\rho_{22} = (aA_1 R_1(E_1))^2 + (bA_4 R_2(E_4))^2 - 2A_1 A_4$$
$$\times ab R_1(E_1)R_2(E_4)\cos((E_1 - E_4)t)F_{14},$$

$$\rho_{22} = \rho_{33} = \rho_{23},$$

$$\rho_{14} = -R_2(E_1)(aA_1)^2 - R_1(E_4)(bA_4)^2$$
$$+ A_1 A_4 ab\exp(-i(E_1 - E_4)t)F_{14}$$
$$- A_1 A_4 R_1(E_1)R_2(E_4)ab$$
$$\times \exp(-i(E_4 - E_1)t)F_{14}$$

$$\rho_{41} = \rho_{14}^*,$$

$$\rho_{44} = (aA_1 R_2(E_1))^2 + (bA_4)^2 - 2A_1 A_4$$
$$\times ab R_2(E_1)\cos((E_1 - E_4)t)F_{14}.$$

$$R_1(E_j) = (\varepsilon_m - \varepsilon - E_j)/2\beta,$$

$$R_2(E_j) = (\varepsilon_m - \varepsilon - E_j)/(\varepsilon_m + \varepsilon - E_j),$$

$$R_3(E_j) = 2\beta/(\varepsilon_m + \varepsilon - E_j); \ j = 1, 2, 3, 4$$

$$A_1 = \frac{1}{\sqrt{1 + 2R_1^2(E_1) + R_2^2(E_1)}},$$

$$A_1 = \frac{1}{\sqrt{1 + 2R_1^2(E_1) + R_2^2(E_1)}},$$

$$A_3 = \frac{1}{\sqrt{2 + R_1^2(E_3) + R_3^2(E_3)}},$$

$$A_4 = \frac{1}{\sqrt{1 + 2R_1^2(E_4) + R_2^2(E_4)}}$$

2.2. Double Majorana wires (DMWs)

We investigate the additional feature prevailed by non-locality of the low lying Majorana modes when they are capacitively and purely coupled between adjacent island when teleporting quantum states i.e. short distance quantum teleportation in quantum networks (figure 2).

In this case there is entanglement hoping in alternate site, i.e. the double Majorana end modes plays the role of electron sites as seen from the Kitaev chain model. The two sites each
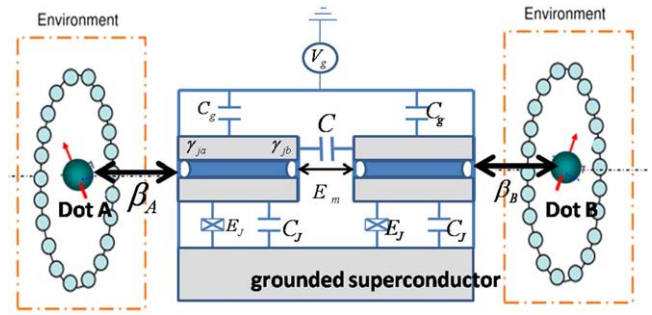
Figure 2. Schematic setup to probe teleportation mediated by double Marjorana wires between two remote dots (qubits) interacting in the same manner with respective spin environments. The Majorana zero modes are represented by white dots. The tunnel coupling of individual electrons between the superconducting islands is proportional to the energy scale E_M. A common gate voltage V_g can be used to tune the relative strength of the different terms in the Hamiltonian. The capacitive couplings between the elements are denoted by C, C_J and C_g, respectively as defined in [29].

support a MBs. The Hamiltonian of the total system mapping into effective spin model reads

$$H_2 = \tilde{H}_{\text{sys}} + H_I, \tag{11}$$

where

$$\tilde{H}_{\text{sys}} = H_0 + H_{\text{ANNNI}}, \tag{12}$$

$$H_0 = \frac{\varepsilon_A}{2}\sigma_A^z + \frac{\varepsilon_B}{2}\sigma_B^z + \beta_A\sigma_A^y\tau_1^y + \beta_B\sigma_B^y\tau_2^y, \tag{13}$$

$$H_{\text{ANNNI}} = \sum_{j=1}^{N}(\Delta\tau_j^z + U\tau_j^z\tau_{j+1}^z + E_m\tau_j^x\tau_{j+1}^x). \tag{14}$$

The sub-system Hamiltonian, $\tilde{H}_{\text{sys}}$ equation (12) constitutes the transverse axial next-nearest-neighbor Ising (ANNNI) model [17]. Detailed derivation of equation (14) is found in [29]. We only give meaning to the parameters entering the Hamiltonian; U introduces additional capacitance between adjacent island that leads to an effective interaction between the low-energy Majorana degrees of freedom. E_M, is pure Majorana coupling between adjacent island or Majorana sites. In our DMW representation, we have two sites, with one site occupied by each wire. From here the Hamiltonian equation (14) becomes; $H_{\text{ANNNI}} = \Delta\tau_1^z + \Delta\tau_2^z + U\tau_1^z\tau_2^z + E_m\tau_1^x\tau_2^x$. The parameters Δ and U can be directly tuned through the induced charge q on the islands via a common back gate voltage V_g. H_I, describes the interaction between the two-qubit spins and the spin chain as discussed in equation (5).

In the same reasoning as in section 2.1, the reduced density matrix after tracing the environmental degrees of freedom is given as

$$\overline{\rho}(t) = \sum_{m,n,\mu,\nu=1}^{8} C_\mu^m \overline{C}_\nu^{*n} F_{mn}(t)|\varphi_\mu\rangle\langle\varphi_\nu|, \tag{15}$$

where

$\overline{C}_\mu^m = \exp(-i\overline{E}_\mu t)\langle\overline{\varphi}_\mu|\overline{\phi}_m\rangle\langle\overline{\phi}_m|\overline{\Phi}\rangle$ and $\overline{C}_\nu^{*n} = \exp(i\overline{E}_\nu t)$ $\langle\overline{\Phi}|\overline{\phi}_n\rangle\langle\overline{\phi}_n|\overline{\varphi}_\nu\rangle$. $\overline{E}_\mu$ corresponds to the eigen-value of the system Hamiltonian $\tilde{H}_{\text{sys}}$. Considering the basis states of the

dot-MBSs–MBSs-dot spin configuration: $|1101\rangle$, $|1011\rangle$, $|1110\rangle$, $|0111\rangle$, $|1000\rangle$, $|0001\rangle$, $|0100\rangle$, $|0010\rangle$, the corresponding eigen-states, may take the general form

$$
\begin{aligned}
|\overline{\phi}_{\mu}\rangle &= a_{\mu}|1101\rangle + b_{\mu}|1011\rangle + c_{\mu}|1110\rangle \\
&+ d_{\mu}|0111\rangle + e_{\mu}|1000\rangle + f_{\mu}|0001\rangle \\
&+ g_{\mu}|0100\rangle + h_{\mu}|0010\rangle,
\end{aligned}
\tag{16}
$$

where, $\mu = 1...8$. The coefficients in equation (15) are obtained when deriving the eigen vectors of the Hamiltonian equation (13).

The eigen states, $|\overline{\phi}_{m}\rangle$: $|1101\rangle$, $|1011\rangle$, $|1110\rangle$, $|0111\rangle$, $|1000\rangle$, $|0001\rangle$, $|0100\rangle$, $|0010\rangle$, are those of the interaction Hamiltonian, H_I between the remote two-qubit spins and the spin chain. The dressed eigen-values are:

$$
\overline{\lambda}_{1(2)} = \lambda + g, \quad \overline{\lambda}_{3,4,5,6} = \lambda, \quad \overline{\lambda}_{7(8)} = \lambda - g.
\tag{17}
$$

The absolute value of the decoherence factors are

$$
|\overline{F}_{mn}| = \prod_{k \succ 0} \left\{
\begin{aligned}
&1 - \sin^2\left(2\overline{\alpha}_k^{\overline{\lambda}_m}\right)\sin^2\left(\overline{\Omega}_k^{\overline{\lambda}_m}t\right) \\
&- \sin^2\left(2\overline{\alpha}_k^{\overline{\lambda}_n}\right)\sin^2\left(\overline{\Omega}_k^{\overline{\lambda}_n}t\right) \\
&+ 2\sin\left(2\overline{\alpha}_k^{\overline{\lambda}_m}\right)\sin\left(\overline{\Omega}_k^{\overline{\lambda}_m}t\right)\sin\left(\overline{\Omega}_k^{\overline{\lambda}_n}t\right) \\
&\times \sin\left(\overline{\Omega}_k^{\overline{\lambda}_n}t\right)\cos\left(\overline{\Omega}_k^{\overline{\lambda}_m}t - \overline{\Omega}_k^{\overline{\lambda}_n}t\right) \\
&- 4\sin\left(2\overline{\alpha}_k^{\overline{\lambda}_m}\right)\left(2\overline{\alpha}_k^{\overline{\lambda}_n}\right)\sin^2\left(\overline{\alpha}_k^{\overline{\lambda}_m} - \overline{\alpha}_k^{\overline{\lambda}_n}\right) \\
&\times \sin^2\left(\overline{\Omega}_k^{\overline{\lambda}_m}t\right)\sin^2\left(\overline{\Omega}_k^{\overline{\lambda}_n}t\right)
\end{aligned}
\right\}^{\frac{1}{2}},
\tag{18}
$$

where

$$
\overline{\Omega}_k^{(\overline{\lambda}_j)} = 2\sqrt{(\varepsilon_k^{(\overline{\lambda}_j)})^2 + \alpha^2 \sin^2 \frac{2\pi k}{N}}; \quad \overline{\varepsilon}_k^{(\overline{\lambda}_j)} = \overline{\lambda}_j - \cos\frac{2\pi k}{N};
$$

$$
\alpha_k^{(\lambda_j)} = (\theta_k^{(\lambda_j)} - \theta_k^{(\lambda)})/2
$$

$$
\cos\overline{\theta}_k^{(\lambda_j)} = 2\overline{\varepsilon}_k^{(\lambda_j)}/\overline{\Omega}_k^{(\lambda_j)}.
\tag{19}
$$

Without lost of insight of the general physics, we consider the initial spin configuration of the dot-MBSs–MBSs-dot system to be in the following arbitrary superposition of state: $|\overline{\Phi}\rangle = \overline{a}|1101\rangle + \overline{b}|1011\rangle + \overline{c}|0100\rangle + \overline{d}|0010\rangle$, with coefficients satisfying: $(\overline{a})^2 + (\overline{b})^2 + (\overline{c})^2 + (\overline{d})^2 = 1$. Tracing over the degrees of freedom of the MFs the reduced density matrix in the standard basis $\{|00\rangle, |01\rangle, |10\rangle, |11\rangle\}$ takes the X-form as

$$
\overline{\rho}_{AB}(t) = \begin{pmatrix} \overline{\rho}_{11} & 0 & 0 & \overline{\rho}_{14} \\ 0 & \overline{\rho}_{22} & \overline{\rho}_{23} & 0 \\ 0 & \overline{\rho}_{32} & \overline{\rho}_{33} & 0 \\ \overline{\rho}_{14}^* & 0 & 0 & \overline{\rho}_{44} \end{pmatrix},
\tag{20}
$$

where

$$
\overline{\rho}_{11}(t) = \sum_{m,n,\mu,\nu=1}^{8} \overline{C}_{\mu}^{m}\overline{C}_{\nu}^{*n}(h_{\mu}h_{\nu} + g_{\mu}g_{\nu})|\overline{F}_{mn}(t)|,
$$

$$
\overline{\rho}_{22}(t) = \sum_{m,n,\mu,\nu=1}^{8} \overline{C}_{\mu}^{m}\overline{C}_{\nu}^{*n}(f_{\mu}f_{\nu} + c_{\mu}c_{\nu})|\overline{F}_{mn}(t)|,
$$

$$
\overline{\rho}_{33}(t) = \sum_{m,n,\mu,\nu=1}^{8} \overline{C}_{\mu}^{m}\overline{C}_{\nu}^{*n}(e_{\mu}e_{\nu} + d_{\mu}d_{\nu})|\overline{F}_{mn}(t)|,
$$

$$
\overline{\rho}_{44}(t) = \sum_{m,n,\mu,\nu=1}^{8} \overline{C}_{\mu}^{m}\overline{C}_{\nu}^{*n}(b_{\mu}b_{\nu} + a_{\mu}a_{\nu})|\overline{F}_{mn}(t)|,
$$

$$
\overline{\rho}_{23}(t) = \sum_{m,n,\mu,\nu=1}^{8} \overline{C}_{\mu}^{m}\overline{C}_{\nu}^{*n}(f_{\mu}e_{\nu} + d_{\mu}c_{\nu})|\overline{F}_{mn}(t)|
$$

$$
\overline{\rho}_{32}(t) = \overline{\rho}_{23}^*(t),
$$

$$
\overline{\rho}_{14}(t) = \sum_{m,n,\mu,\nu=1}^{8} \overline{C}_{\mu}^{m}\overline{C}_{\nu}^{*n}(h_{\mu}b_{\nu} + g_{\mu}a_{\nu})|\overline{F}_{mn}(t)|,
$$

$$
\overline{\rho}_{41}(t) = \overline{\rho}_{14}^*.
\tag{21}
$$

The decoherence factors in equations (9) and (18) can be consider as the amplitude of overlap of the different states of the spin environment for $\lambda_j \neq \lambda_{j'}(\overline{\lambda}_j \neq \overline{\lambda}_{j'})$ as a result of the interaction between the remote qubits and the spin environment. This interaction introduces overlap of the different bases of the system. The diagonal elements of the system Hamiltonian are not influence by the decoherence factors as it has a value equal to unity for $j = j'$. We seek to evaluate the extent to which a quantum state to be teleported is influenced by these decoherence factors observed at the sending and the receiving locations taking into account non-locality between the two locations.

3. Entanglement teleportation and average fidelity

Having obtained the reduced density matrix for the two systems, we turn to look on quantum quantifiers of correlations between the distant dots and the quality of information transfer. In this illumination, use is made of the entanglement, entanglement teleportation and the average fidelity of the teleported state using two copies of the single and double Majorana wire(s) respectively as quantum bridges.

The entanglement dynamics of the SMW can be calculated from the time dependent density matrix $\rho_{AB}(t)$ of the system using Wootters concurrence [32], as

$$
C(\rho_{AB}(t)) = \max\{0, \sqrt{\varpi_1} - \sqrt{\varpi_2} - \sqrt{\varpi_3} - \sqrt{\varpi_4}\},
\tag{22}
$$

where the quantities ϖ_i are roots of the eigenvalues in decreasing order of the auxiliary matrix $\varsigma = \rho_{AB}(t)(\sigma_y \otimes \sigma_y)\rho_{AB}^*(t)(\sigma_y \otimes \sigma_y)$. $\rho_{AB}^*(t)$ denotes the complex conjugate of $\rho_{AB}(t)$ in the standard bases and σ_y is the Pauli matrix. The evaluation of concurrence gives

$$
\begin{aligned}
C(\rho_{AB}(t)) = \max\{&\sqrt{\rho_{11}\rho_{44}} + |\rho_{14}| \\
&- |\sqrt{\rho_{11}\rho_{44}} - |\rho_{14}|| - 2\rho_{22}\}.
\end{aligned}
\tag{23}
$$

We consider the two qubit teleportation protocol proposed by Lee and Kim, using two copies of the system figures 1 and 2 for the two configurations. We study the effects of the environment and the channel parameters on the entanglement, entanglement teleportation and average fidelity.

Without loss of generality we consider the input state to be teleported to be the general state:

$$|\psi_{\text{in}}\rangle = \cos\frac{\theta}{2}|10\rangle + e^{i\varphi}\sin\frac{\theta}{2}|01\rangle,$$
$$(0 \leqslant \theta \leqslant \pi \text{ and } 0 \leqslant \phi \leqslant 2\pi), \qquad (24)$$

where θ represent the amplitude and ϕ represents the phase of the input state. The density matrix related to the input state $|\psi_{\text{in}}\rangle$ is

$$\rho_{\text{in}} = |\psi_{\text{in}}\rangle\langle\psi_{\text{in}}|. \qquad (25)$$

The output state can be obtained by applying joint measurements and local unitary transformations on the input state ρ_{in}. Following the teleportation protocol proposed by Lee and Kim output state of the two qubit teleportation can be written as

$$\rho_{\text{out}} = \sum_{i,j} P_{ij}(\sigma^i \otimes \sigma^j)\rho_{\text{in}}(\sigma^i \otimes \sigma^j), \qquad (26)$$

where $i, j = 0, 1, 2, 3$, $\sigma^0 = I$ (identity 2×2 matrix), while $\sigma^1 = \sigma^x$, $\sigma^2 = \sigma^y$, and $\sigma^3 = \sigma^z$ are Pauli Matrices.

The probabilities $P_{ij} = P_i P_j$ satisfy the condition $\sum_{i,j} P_{ij} = 1$

with

$$P_j = \text{Tr}\{E^j \rho_{\text{channel}}\} \qquad (27)$$

Here $\rho_{\text{channel}} = \rho_s(t) = \begin{pmatrix} \rho_{11} & 0 & 0 & \rho_{14} \\ 0 & \rho_{22} & \rho_{23} & 0 \\ 0 & \rho_{32} & \rho_{33} & 0 \\ \rho_{14}^* & 0 & 0 & \rho_{44} \end{pmatrix}$ is the reduced

density matrix of the two qubits at the remote ends of the wire and serves as our quantum channel. The projective measurements E^j are defined from the four maximally entangled Bell states as follows:

$$E^0 = |\psi^-\rangle\langle\psi^-|, \ E^1 = |\phi^-\rangle\langle\phi^-|, \ E^2 = |\phi^+\rangle\langle\phi^+|,$$
$$E^3 = |\psi^+\rangle\langle\psi^+| \qquad (28)$$

with the maximally entangled bell states given by

$$|\psi^\pm\rangle = \frac{1}{\sqrt{2}}(|01\rangle \pm |10\rangle), \ |\phi^\pm\rangle = \frac{1}{\sqrt{2}}(|00\rangle \pm |11\rangle). \qquad (29)$$

After a straight evaluation of equation (26) we obtain the

density matrix of the output states of the form

$$\rho_{\text{out}} = \begin{pmatrix} u & 0 & 0 & v \\ 0 & w & x & 0 \\ 0 & x^* & y & 0 \\ v & 0 & 0 & u \end{pmatrix}, \qquad (30)$$

where we have:

$$u = 2\rho_{22}(\rho_{11} + \rho_{44}),$$
$$v = 2\rho_{22}(\rho_{14}^* + \rho_{14})\sin\theta\cos\phi,$$
$$w = 4\sin^2\left(\frac{\theta}{2}\right)(\rho_{22})^2 + \cos^2\left(\frac{\theta}{2}\right)(\rho_{11} + \rho_{44})^2,$$
$$x = \frac{1}{2}e^{i\phi}\sin\theta(4\rho_{22}^2) - \frac{1}{2}e^{-i\phi}\sin\theta(\rho_{14}^* + \rho_{14})^2,$$
$$y = 4\cos^2\left(\frac{\theta}{2}\right)(\rho_{22})^2 + \sin^2\left(\frac{\theta}{2}\right)(\rho_{11} + \rho_{44})^2. \qquad (31)$$

We now evaluate the concurrence of the output state and we find that it can be expressed as

$$C_{\text{out}} = \max\{\zeta_1 - \zeta_2 - \zeta_3 - \zeta_4, 0\}, \qquad (32)$$

where $\zeta_1 \geqslant \zeta_2 \geqslant \zeta_3 \geqslant \zeta_4$ are the square roots in order of decreasing magnitude of the eigen values of the operator

$$R' = \rho_{\text{out}}(\sigma^y \otimes \sigma^y)\rho_{\text{out}}^*(\sigma^y \otimes \sigma^y). \qquad (33)$$

The quantities in equation (32) ζ_1, ζ_2, ζ_3 and ζ_4 are given as:
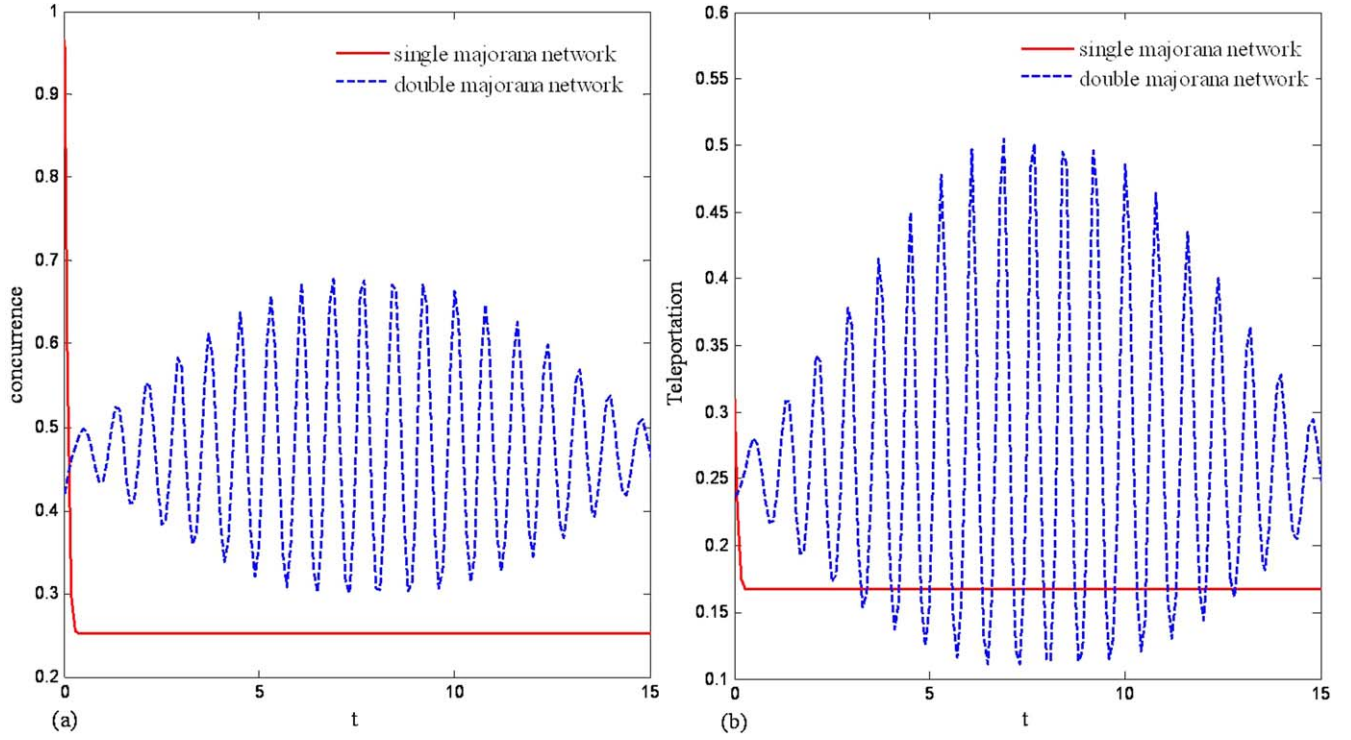
$$\zeta_1^2 = |x|^2 + wy^* + |x|\sqrt{(w + w^*)(y + y^*)},$$
$$\zeta_2^2 = |x|^2 + wy^* - |x|\sqrt{(w + w^*)(y + y^*)},$$
$$\zeta_3^2 = |u|^2 + |v|^2 + uv^* + vu^*,$$
$$\zeta_4^2 = |u|^2 + |v|^2 - uv^* - vu^*. \qquad (34)$$

As there must be quantification of the quality of the information transfer, use is made of the figure of merit called the fidelity [33, 34]. It is an important tool to characterize the closeness of any two mixed states, and often used in modern applications of quantum mechanics. It is equal to unity if and only if both states do coincide. The fidelity between the input state and the output state for our system is defined by [34]

$$F(\rho_{\text{in}}, \rho_{\text{out}}) = \left\{\text{Tr}\left(\sqrt{(\rho_{\text{in}})^{\frac{1}{2}}\rho_{\text{out}}(\rho_{\text{in}})^{\frac{1}{2}}}\right)\right\}^2. \qquad (35)$$

Considering the density matrices of the input state ρ_{in} and the output state ρ_{out}, the fidelity of the teleportation is obtained as

$$F(\rho_{\text{in}}, \rho_{\text{out}}) = \left\{ \begin{array}{l} \left(\sqrt{\sin^2\left(\frac{\theta}{2}\right)w + \sin\left(\frac{\theta}{2}\right)\left(\frac{\sin\theta}{2}\right)^{\frac{1}{2}}(e^{\frac{i\varphi}{2}}x^* + e^{\frac{-i\varphi}{2}}x) + \frac{1}{2}(\sin\theta)y}\right) \\ + \left(\sqrt{\sin^2\left(\frac{\theta}{2}\right)w + \cos\left(\frac{\theta}{2}\right)\left(\frac{\sin\theta}{2}\right)^{\frac{1}{2}}(e^{\frac{i\varphi}{2}}x^* + e^{\frac{-i\varphi}{2}}x) + \frac{1}{2}(\cos^2\theta)y}\right) \end{array} \right\}^2. \qquad (36)$$

Figure 3. Comparative study on the dynamics of (a) entanglement (b) entanglement teleportation, for the single Majorana wire and double Majorana wires for a weakly coupled dots-spin environment, $g = 0.05$. Other parameters are set to: $\varepsilon = 0.1$, $\beta = 0.1$, $\varepsilon_m = 0.01$, $\Delta = U = E_m = 0.01$, $\lambda = 1$, $\alpha = 0.1$, $N = 101$.

Replacing the values of w, x and, y we can write the fidelity as:

$$F(\rho_{\text{in}}, \rho_{\text{out}}) = 4\rho_{22}^2 + \sin^2\theta\{4\rho_{14}\rho_{14}^* \cos(2\phi) + (\rho_{11} + \rho_{44})^2\}. \tag{37}$$

To efficiently measure the quality of the protocol, we calculate the average fidelity between the input and output states by averaging over all possible input states. Under the influence of the environment and channel parameters, the maximally entangled component can vary with time. Therefore, the best quality of the teleportation can be obtained by the optimal estimation of the projective measurements. Thus the average fidelity will be a function of time. The average fidelity is defined from the fidelity as

$$F_A(t) = \frac{1}{4\pi} \int_0^{2\pi} \mathrm{d}\phi \int_0^\pi F(\rho_{\text{in}}, \rho_{\text{out}}) \sin\theta \mathrm{d}\theta. \tag{38}$$

We obtain the average fidelity as

$$F_A(t) = 4\rho_{22}^2 + \frac{2}{3}(\rho_{11} + \rho_{44})^2. \tag{39}$$

In the same setting, the expressions of concurrence and entanglement teleportation for the DMWs are as follows

$$\overline{C}(\rho_{AB}(t)) = \max\{\sqrt{\overline{\rho}_{11}\overline{\rho}_{44}} + |\overline{\rho}_{14}| - |\sqrt{\overline{\rho}_{11}\overline{\rho}_{44}} - |\overline{\rho}_{14}|| - 2\overline{\rho}_{22}\}, \tag{40}$$

$$\overline{F}(\rho_{\text{in}}, \rho_{\text{out}}) = 4\overline{\rho}_{22}^2 + \sin^2\theta\{4\overline{\rho}_{14}\overline{\rho}_{14}^* \cos(2\phi) + (\overline{\rho}_{11} + \overline{\rho}_{44})^2\}. \tag{41}$$

4. Results and discussions

In figure 3(a) we provide a comparative study of the role of the spin environment weakly coupled to the two remote qubits on entanglement dynamics for the SMW and the DMWs. It is observed that entanglement drops so quickly and later achieves an asymptotic behavior for the SMW while for the DMWs, there is enhancement in entanglement with characteristic cyclic beating. In the same setting, we noticed a similar trend in the dynamics of entanglement teleportation figure 3(b).

We carried out the same comparative studies but in the opposite end of strongly coupled spin environment with the remote qubits for the entanglement dynamics figure 4(a) and the dynamics of the teleported state figure 4(b). Entanglement for the SMW (red solid curve) drops noisily during the first periods of its dynamics and later observes a quasi-periodic death and revival during the long time dynamics (see insert figure 4(a)). The strong coupling between the spin environment and the qubits leads to strong quantum fluctuations in the qubits which in turn are observed by the MBS (as seen from the noisy oscillations). The qubits strong quantum fluctuations remove the zero-energy MBs by driving the system through a topological quantum phase [35] characterized by the closing of the energy gap at the topological critical
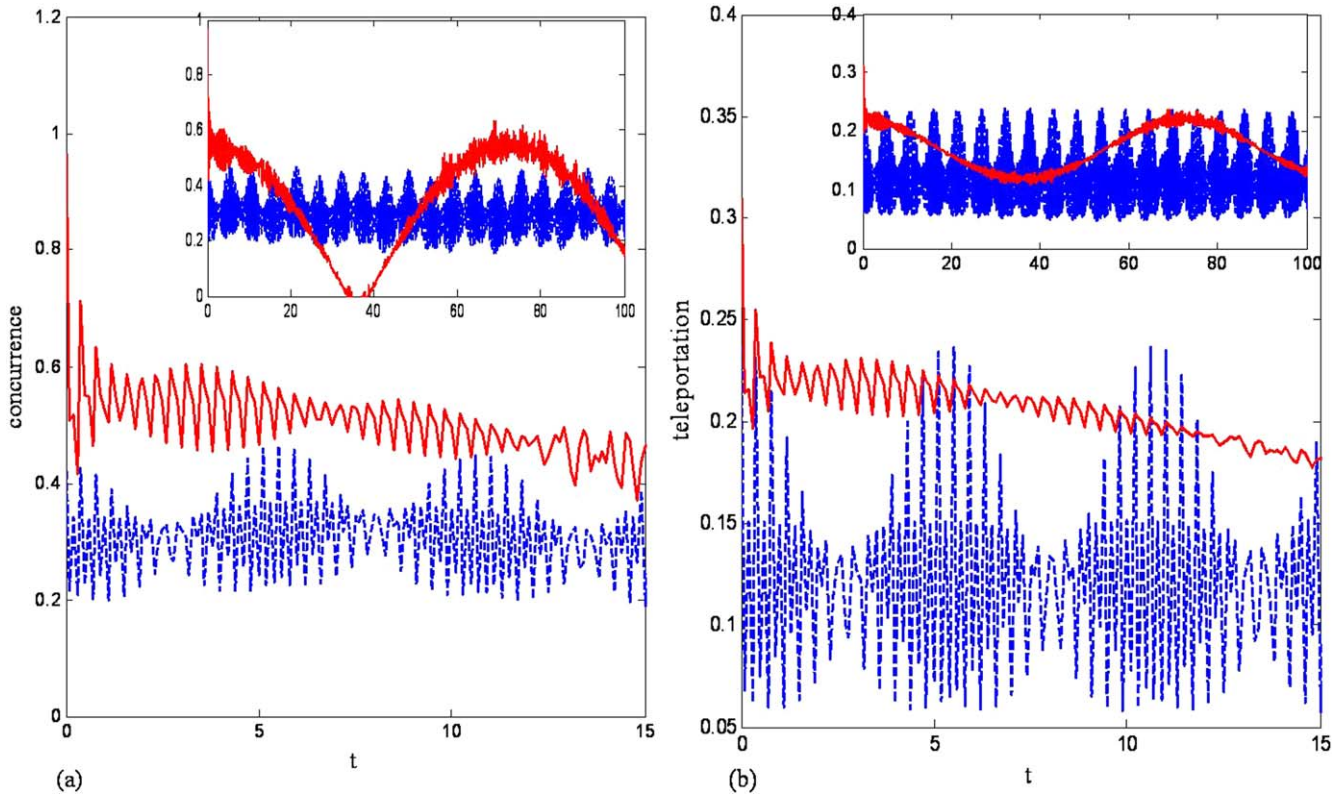
Figure 4. Comparative study on the dynamics of (a) entanglement (b) entanglement teleportation, for the SMW (red solid line) and DMWs (blue dash line) for a strongly coupled dots-spin environment, $g = 10$. The inserts in plots (a) and (b) are for the long time dynamics. Other parameters are set to: $\varepsilon = 0.1$, $\beta = 0.1$, $\varepsilon_m = 0.01$, $\Delta = U = E_m = 0.01$, $\lambda = 1$, $\alpha = 0.1$, $N = 101$.

point where MFs become entangled with other gapless states [36]. The manifestation of periodic death and revival in the entanglement dynamics arises from the memory effects of the spin bath.

The dynamics for the DMWs (blue dash curve) beats rapidly and cyclically. A similar trend is observed in the dynamics of entanglement teleportation (figure 4(b)) for both configurations with the difference that no death and revival is observed for the SMW. For the parameter space considered in both coupling regimes, the DMWs seems to show a better entanglement router than the SMW as the former seems robust to the fluctuating action of the spin environment coupled to the qubits. This behavior as seen from the cyclic beating phenomenon stems from the fact that the DMWs is endowed with the trivial phases and the topological phases which serves as channels for routing information. The presence of these phases has been observed in the general form of the spin model Hamiltonian equation (16) for $j = 1 \rightarrow N$ [29]. The topological phase includes the anti-ferromagnetic phase (AF) and two degenerate ground states. The presence of the AF-phase marches well with the report given in [5, 7] where perfect entanglement transfer over arbitrary long distance is achieved for an AF spin chain than for the ferromagnetic spin chain. These inherent features boost information transfer in the DMWs setting.

In figure 5, we investigate the influence of the coupling between dots and Majorana for an arbitrary coupling strength between dots and spin environment on the teleported state.

For the SMW configuration (figure 5(a)), the teleportation dynamics observes an asymptotic stable increase for very small dot-Majorana coupling and asymptotic stable decrease as we increase the dot-Majorana coupling. For the DMWs configuration figure 5(b), we see that there exists a critical value of the dot-Majorana coupling where the entanglement dynamics is maximum. Reducing the coupling increases the entanglement teleportation up to a maximum value after which it reduces when further increasing the coupling.

This suggests that there exist a critical point where the coupling between the dots and the MFs drives the SMW configuration to a topological quantum phase transition and to other topological phases for the DMWs configuration. The peak value (figure 6) should correspond to the topological phase that features the MFs. We note that the DMWs imitate the behavior of the SMW.

Figure 7 shows that the dynamics of entanglement teleportation is almost insensitive to the number of atoms after a short while for the DMWs figure 7(a) and the SMW figure 7(b). This contradicts the fact that for an exchange coupled spin configuration the dynamics of quantum correlations decrease as the number of bath atoms increases [31]. This is one of the reasons why at zero temperatures the spin environment effects are dominated by localized modes rather than the size of the environment. Using MFs to teleport quantum state(s), this scenario is observed. We would like to report that, in one of our research paper, we show that
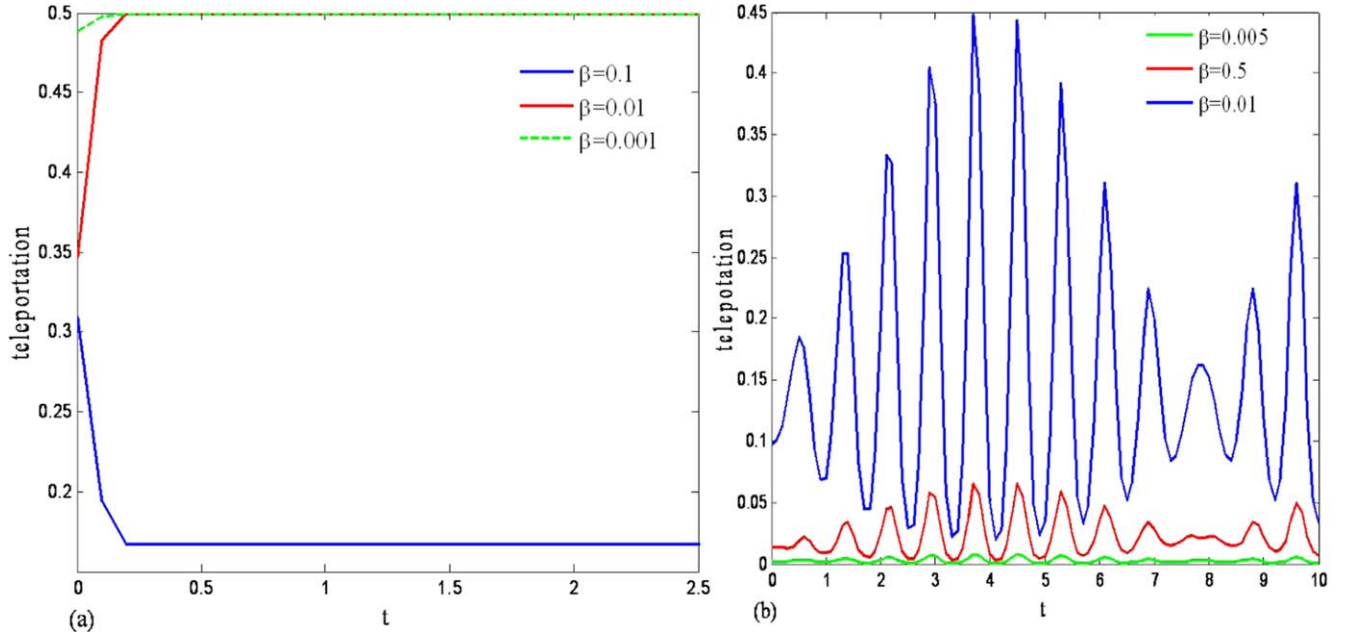
Figure 5. Dynamics of entanglement teleportation (a) single Majorana wire (b), double Majorana wires, for different coupling between dots and Majorana, β. Other parameters are set to: $\varepsilon = 0.1$, $N = 101$, $\varepsilon_m = 0.01$, $\Delta = U = E_m = 0.01$, $\lambda = 1$, $g = 0.10$, $\alpha = 0.1$.
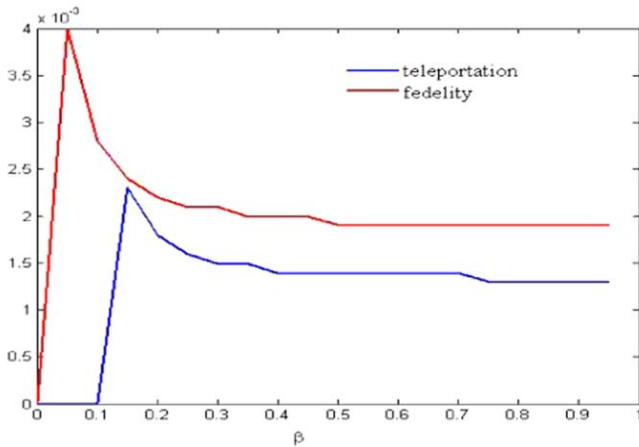
Figure 6. Plot of the variation of entanglement teleportation and average fidelity as β is varied for the double Majorana wires. Other parameters are set to: $\varepsilon = 0.1$, $\varepsilon_m = 0.01$, $\Delta = U = E_m = 0.01$, $\lambda = 1$, $g = 0.10$, $\alpha = 0.1$, $N = 101$.

quantum correlations and fidelity are influenced by the spin model.

The role of the capacitive coupling on the DMWs is investigated in figure 8. We generally noticed that small values of the capacitive coupling, enhances entanglement dynamics figure 8(a), and the dynamics of entanglement teleportation figure 8(b). The same trend is observed when varying the pure coupling between the two Majorana island figure 9. This implies very small values of the capacitive coupling and coupling between Majorana island are necessary for entanglement generation between the two sites featuring the Majorana zero modes while large values could drive the

system to Mott insulator characterized by the Floating phase and the Anti-phase [29] thus destroying the topological phases that accommodate entanglement generation.

5. Conclusion

This work investigates the decoherence effects on the teleportation of entanglement between distinct qubits embedded in a spin environment using a single and double Majorana wire(s) respectively as quantum channels or data buses. The role of the composite system parameters on entanglement, entanglement teleportation and average fidelity are examined. The sensitivity of the teleported state on the different coupling regimes between the spin environment and qubits are established. Our results show that strong coupling between the spin environment and the qubits modifies the coupling between the qubits and the MFs thus lifting the degenerate zero energy state for the case of the SMW. The SMW is seen to undergo a topological quantum phase transition as seen from the stable asymptotic increase and decrease in its dynamics as the coupling between the qubits and the MFs are varied. To achieve better transmission of information, optimal engineering of the coupling between the qubits and the MBs is required for both channels irrespective of the decoherence effect from the sending and the receiving host spin environment. While the SMW configuration is prone to the environmental quantum fluctuations, the DMWs configuration is robust as observed from the coherent cyclic beating in its dynamics. We attribute the cyclic beating as coherent leakage of information between the topological and the AFM phases. We also observed that large values of capacitive coupling and coupling between Majorana islands destroys entanglement generation between the two sites and thus decrease in the
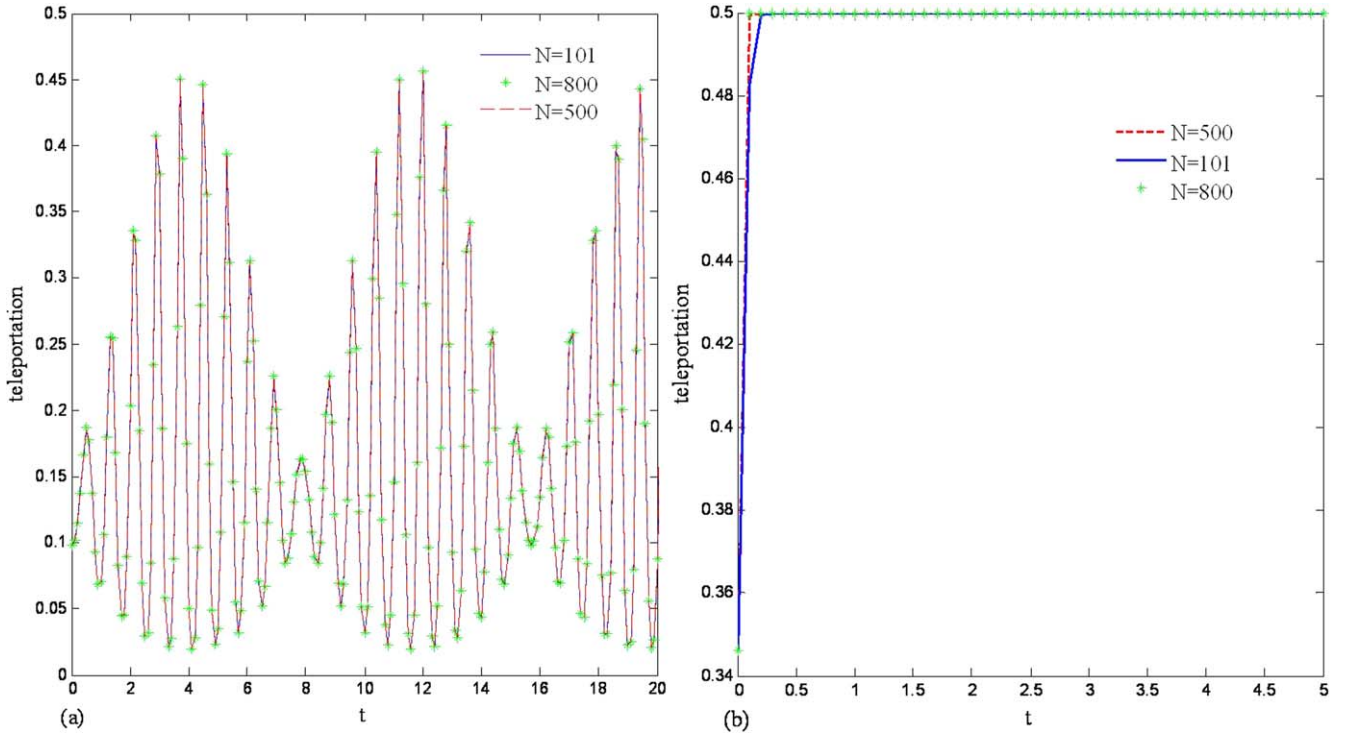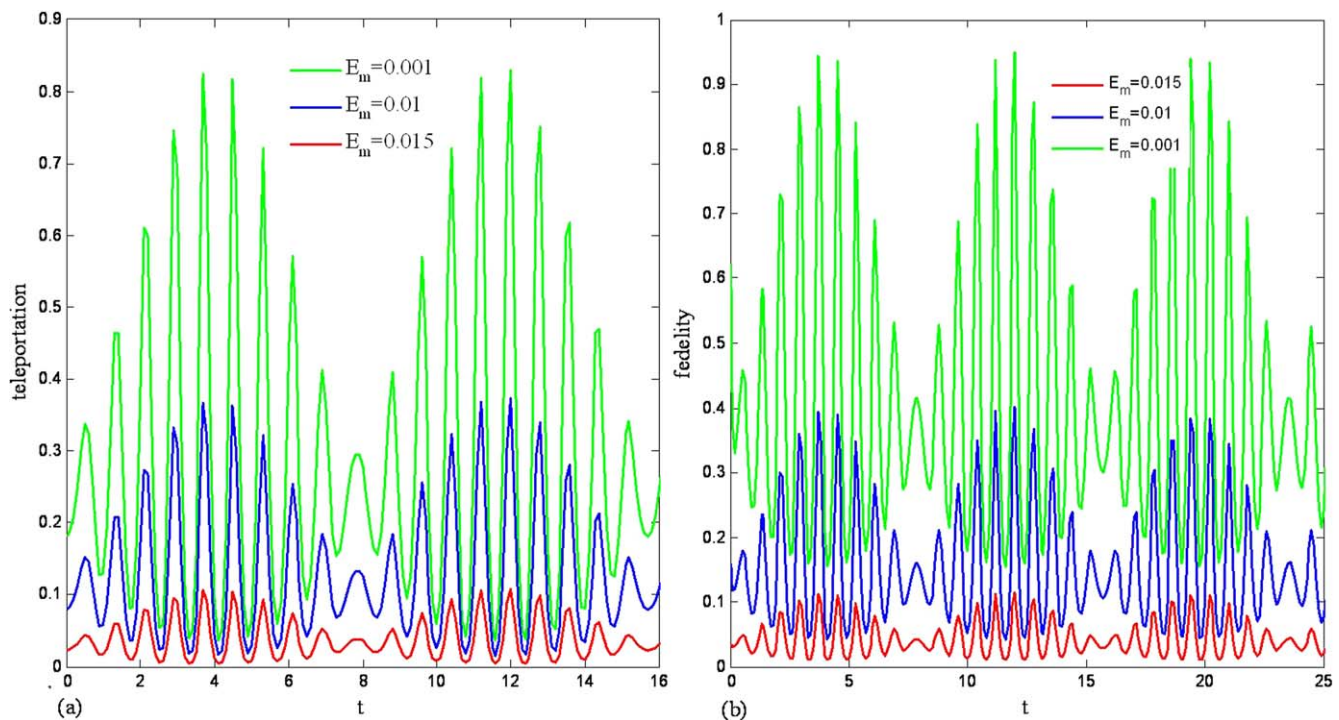
Figure 7. Dynamics of entanglement teleportation for (a) double Majorana wires (b) single Majorana wire, for different number of atoms. Other parameters are set to: $\varepsilon = 0.1$, $\beta = 0.1$, $\varepsilon_m = 0.01$, $\Delta = U = E_m = 0.01$, $\lambda = 1$, $g = 0.10$, $\alpha = 0.1$.
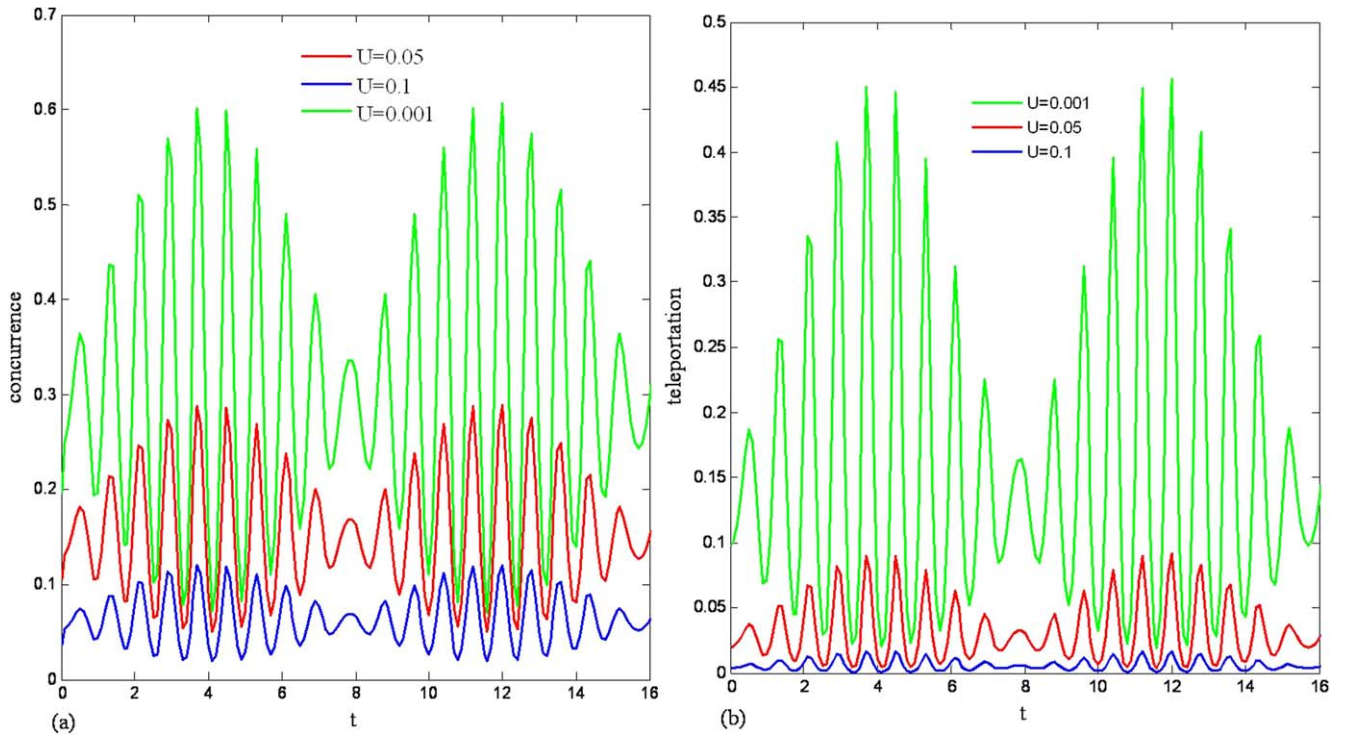
Figure 8. Dynamics of (a) entanglement (b) entanglement teleportation for the double Majorana wires as the capacitative coupling is varied, U. Other parameters are set to: $\varepsilon = 0.1$, $\beta = 0.01$, $\varepsilon_m = 0.01$, $\Delta = E_m = 0.01$, $\lambda = 1$, $\alpha = 0.1$, $g = 1$, $N = 101$.

fidelity of quantum state transfer. In the whole, to have better entanglement, entanglement of the teleported state and the average fidelity of the teleported state in a decohered environment, we need optimal engineering of the parameter space of the composite system Hamiltonian such that the topological phase that features MFs could be accessed.

Figure 9. Dynamics of (a) entanglement teleportation (b) average fidelity for the double Majorana wires as the pure coupling is varied, E_m. Other parameters are set to: $\varepsilon = 0.1$, $\beta = 0.01$, $\varepsilon_m = 0.01$, $\Delta = U = 0.01$, $\lambda = 1$, $\alpha = 0.1$, $g = 1$, $N = 101$.

Acknowledgments

ORCID iDs

Ngwa Engelbert Afuoti ⬤ https://orcid.org/0000-0002-4295-9370

References

[1] Bose S 2003 Quantum computation through un-modulated spin chain *Phys. Rev. Lett.* **91** 207901–4

[2] Subrahmanyam V 2004 Entanglement dynamics and quantum state transport in spin chain *Phys. Rev.* A **69** 034304–7

[3] Kay A 2007 Unifying quantum state transfer and state amplification *Phys. Rev. Lett.* **98** 010501–4

[4] Eckert K, Romero-Isart O and Sanpera A 2007 Efficient quantum state transfer in spin chain via adiabatic passage *New J. Phys.* **9** 155–73

[5] Sarkar S 2011 Perfect entanglement transport in quantum spin chain systems *J. Quantum Inf. Sci.* **1** 105–10

[6] Yao N Y, Jiang L, Gorshkov A V, Gong Z X, Zhai A, Duan L M and Lukin M D 2011 Robust quantum state transfer in random unpolarized spin chains *Phys. Rev. Lett.* **106** 040505

[7] Bayat A, Burgarth D, Mancini S and Bose S 2007 Memory effects in spin-chain channels for information transmission *Phys. Rev. A* **77** 050306

[8] Kielpinski D, Monroe C and Wineland D J 2002 Architecture for a large-scale ion-trap quantum computer *Nature* **417** 709–11

[9] Duan L M, Blinov B B, Moehring D L and Monroe C 2004 Scalable ion trapped quantum computation with a probabilistic ion-photon mapping *Quantum Inf. Comput.* **4** 165–73

[10] Christodoulides D N, Lederer F and Silberberg Y 2003 Discretizing light behaviour in linear and nonlinear waveguide lattices *Nature* **424** 817–23

[11] Bellec M, Nikolopoulos G M and Tzortzakis S 2012 A faithful communication Hamiltonian in photonic lattices *Opt. Lett.* **37** 4504–6

[12] Kitaev Y A 2003 Fault-tolerant quantum computation by anyons *Ann. Phys., NY* **303** 2–30

[13] Sarm S D, Freedman M and Nayak C 2006 Topological quantum computation *Phys. Today* S-0031-9228-06070-020-7

[14] Sarm S D, Freedman M, Nayak C, Steven H S and Stern A 2008 Non-Abelian anyons and topological quantum computation *Rev. Mod. Phys.* **80** 1083

[15] Nayak C, Steven H S, Stern A, Michael F and Sankar D S 2008 Non-Abelian anyons and topological quantum computation *Rev. Mod. Phys.* **80** 1083

[16] Moore G and Read N 2000 Paired states of fermions in two dimensions with breaking of parity and time reversal symmetries and the fractional quantum Hall effect *Phys. Rev. B* **61** 10267

[17] Kitaev A Y 2001 Unpaired Majorana fermions in quantum wires *Phys.—Usp.* **44** 131–6

[18] Fu L and Kane C 2008 Superconducting proximity effect and Majorana fermions at the surface of a topological insulator *Phys. Rev. Lett.* **100** 096407

[19] Oreg Y, Refael G and von Oppen F 2010 Helical liquids and Majorana bound states in quantum wires *Phys. Rev. Lett.* **105** 177002

[20] Mourik V, Zuo K, Frolov S M, Plissard S R, Bakkers E P A M and Kouwenhoven L P 2012 Signatures of Majorana fermions in hybrid superconductor-semiconductor nanowire devices *Science* **336** 1003–7

[21] Deng M T, Yu C L, Huang G Y, Larsson M, Caroff P and Xu H Q 2014 Parity independence of the zero-bias conductance peak in a nano-wire based topological superconductor-quantum dot hybrid device *Sci. Rep.* **4** 7261

[22] Deng M T, Yu C L, Huang G Y, Larsson M, Caroff P and Xu H Q 2012 Anomalous zero-bias conductance peak in a Nb-InSb nanowire-Nb hybrid device *Nano Lett.* **12** 6414–9

[23] Das A, Ronen Y, Most Y, Oreg Y, Heiblum M and Shtrikman H 2012 Zero-bias peaks and splitting in an Al-InAs nanowire topological superconductor as a signature of Majorana fermions *Nat. Phys.* **12** 887–95

[24] Wang P, Cao Y, Gong M, Li S S and Xin-Qi Li X Q 2013 *Demonstrating Nonlocality Induced Teleportation Through Majorana Bound States in a Semiconductor Nanowire* arXiv:1208.3736V2

[25] Li J, Ting Y T, Lin H Q and You J Q 2014 Probing the non-locality of Majorana fermions via quantum correlations *Sci. Rep.* **4** 4930

[26] Ng H T 2015 Decoherence of interacting Majorana modes *Sci. Rep.* **5** 12530

[27] Wang P, Cao Y, Gong M, Li S S and Xin-Qi Li X Q 2013 Cross-correlations mediated by Majorana bound states *Europhys. Lett.* **103** 57016

[28] Ricco L S *et al* 2018 *Sci. Rep.* **8** 2790

[29] Hassler F and Schuricht D 2012 Strongly interacting Majorana modes in an array of Josephson junctions *New J. Phys.* **14** 125018

[30] Lee J and Kim M S 2000 Entanglement teleportation via werner states *Phys. Rev. Lett.* **84** 4236

[31] Cheng W W and Liu J M 2009 Decoherence from spin environment: role of the Dzyaloshinsky-Moriya interaction *Phys. Rev.* A **79** 052320

[32] William K 1998 Entanglement of formation of an arbitrary state of two qubits *Phys. Rev. Lett.* **80** 2245

[33] Bowen G and Bose S 2001 Teleportation as a depolarizing quantum channel, relative entropy and classical capacity *Phys. Rev. Lett.* **87** 267901

[34] Jozsa R 1994 Fidelity for mixed quantum states *J. Mod. Opt.* **41** 2315–23

[35] Volovik G E 1988 *Zh. Eksp. Teor. Fiz.* **94** 123

[36] Read N and Green D 2000 *Phys. Rev.* B **61** 10267